Eur. Phys. J. D **18**, 155–160 (2002)
DOI: 10.1140/epjd/e20020019

THE EUROPEAN PHYSICAL JOURNAL D
EDP Sciences

PPLN waveguide for quantum communication

S. Tanzilli[1,a], W. Tittel[2], H. De Riedmatten[2], H. Zbinden[2], P. Baldi[1], M. De Micheli[1], D.B. Ostrowsky[1], and N. Gisin[2]

[1] Laboratoire de Physique de la Matière Condensée[b], Université de Nice-Sophia Antipolis, Parc Valrose, 06108 Nice Cedex 2, France
[2] Group of Applied Physics, Université de Genève, 20 rue de l'École-de-Médecine, 1211 Geneva 4, Switzerland

Received 13 July 2001

Abstract. We report on energy-time and time-bin entangled photon-pair sources based on a periodically poled lithium niobate (PPLN) waveguide. Degenerate twin photons at 1 314 nm wavelength are created by spontaneous parametric down-conversion and coupled into standard telecom fibers. Our PPLN waveguide features a very high conversion efficiency of about 10^{-6}, roughly 4 orders of magnitude more than that obtained employing bulk crystals [1]. Even if using low power laser diodes, this engenders a significant probability for creating two pairs at a time – an important advantage for some quantum communication protocols. We point out a simple means to characterize the pair creation probability in case of a pulsed pump. To investigate the quality of the entangled states, we perform photon-pair interference experiments, leading to visibilities of 97% for the case of energy-time entanglement and of 84% for the case of time-bin entanglement. Although the last figure must still be improved, these tests demonstrate the high potential of PPLN waveguide based sources to become a key element for future quantum communication schemes.

PACS. 42.65.Wi Nonlinear waveguides – 03.65.Ud Entanglement and quantum nonlocality (e.g. EPR paradox, Bell's inequalities, GHZ states, etc.) – 03.67.Hk Quantum communication

1 Introduction

Sources creating entangled photon-pairs are an essential tool for a variety of fundamental quantum optical experiments like tests of Bell-inequalities [2–9], quantum teleportation [10–12] and entanglement swapping [13], as well as for more applied fields of research such as quantum cryptography [14–16] and "quantum" metrology [17,18].

To date, the creation of entangled photon-pairs is usually assured by spontaneous parametric down conversion (PDC) in non-linear bulk crystals. However, despite enormous success in the above-mentioned experiments, these sources suffer from low pair production efficiencies. This turns out to be an important limitation, especially if simultaneous creation of two pairs is required as in quantum teleportation [10], entanglement swapping [13], or in present schemes for the realization of GHZ states [19–21]. Taking advantage of integrated optics, we have recently built a new photon-pair source based on a quasi-phase-matched optical waveguide implemented on periodically poled lithium niobate (PPLN)[1]. We previously demonstrated an improvement of the PDC efficiency by 4 orders of magnitude compared to the highest efficiencies reported for bulk crystals [1]. Here, we investigate the quality of the created entanglement in terms of visibilities in two-photon interference experiments for two different PPLN waveguide based sources, the first one producing energy-time entangled photon-pairs, and the second one generating time-bin entanglement.

The article is structured along the following lines: in Section 2, we briefly discuss the advantage and the fabrication of PPLN waveguides. In Section 3, we characterize the efficiency of our source for photon-pair generation by means of coincidence counting experiments based both on a CW and a pulsed pump. The latter turns out to provide a simple means for estimating the probability of creating a photon-pair per pump pulse. Sections 4 and 5 then focus on two different sources creating energy-time entangled as well as time-bin entangled photon-pairs. We investigate the quality of the entanglement via two-photon interference experiments. Finally, we briefly conclude in Section 6.

2 The PPLN waveguide

The interaction of a pump field with a $\chi^{(2)}$ non-linear medium leads, with a small probability, to the conversion of a pump photon into so-called signal and idler photons. Naturally, this process, known as spontaneous parametric down conversion, is subjected to conservation of energy

$$\omega_{\mathrm{p}} = \omega_{\mathrm{s}} + \omega_{\mathrm{i}} \tag{1}$$

[a] e-mail: tanzilli@unice.fr
[b] UMR 6622 du CNRS
[1] See also related work by Sanaka [22].

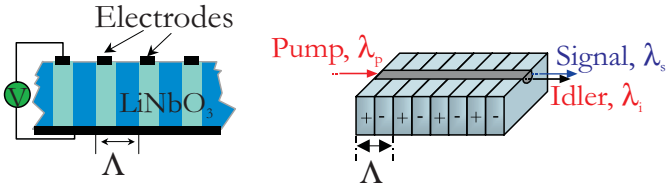

Fig. 1. Poling of the lithium niobate substrate (left hand picture) and schematics of a PPLN waveguide (right hand picture). Λ denotes the poling period, λ_p, λ_s, λ_i are the wavelength for the pump, signal and idler photons, and + and − indicate the sign of the $\chi^{(2)}$ coefficient.

and momentum

$$\mathbf{k}_p = \mathbf{k}_s + \mathbf{k}_i \tag{2}$$

where the indices label the frequency and **k**-vector of the pump, signal and idler fields respectively. The latter equation is also known as the phase-matching condition and can be achieved, despite chromatic dispersion, by employing different polarizations for the three fields (so-called birefringent phase-matching).

In bulk optical configurations, the pump field is often weakly focused into the non-linear crystal and the down-converted photons are then collected into optical fibers by appropriate optics, selecting photons created near the focal point of the first lens. By comparison, the use of a guiding structure permits the confinement of the pump, signal and idler beams over the entire length of the waveguide (a few cm in our case). Therefore, it clearly enables much higher down-conversion efficiencies. However, natural birefringent phase-matching (Eq. (2)) is quite difficult to obtain in a waveguiding structure. A better solution is to employ so-called quasi-phase-matching (QPM) and to integrate the waveguide on a periodically poled lithium niobate (PPLN) substrate, *i.e.* a substrate where the ferroelectric polarization of the material is periodically inverted (see Fig. 1). The resulting phase-matching condition is then given by

$$\mathbf{k}_p = \mathbf{k}_s + \mathbf{k}_i + \mathbf{K} \qquad |\mathbf{K}| = \frac{2\pi}{\Lambda} \tag{3}$$

where **K** represents the effective grating-type **k**-vector and Λ is the poling period. By an appropriate choice of the poling period (Λ), one can quasi-phase-match practically any desired non-linear interaction between the pump, signal and idler fields. In addition to an increased efficiency due to the long interaction length, this allows working with the highest non-linear coefficient of lithium niobate ($d_{33} \approx 30$ pm/V) which is approximately six times larger than that (d_{31}) commonly used in birefringent phase-matching in bulk crystals.

The inversion of the ferroelectric domains is done by applying a high electric field (≈20 kV/mm) periodically on a 500 μm thick lithium niobate sample (see Fig. 1), inducing a periodic flip of the $\chi^{(2)}$ sign.

Once the PPLN substrate is obtained, the waveguide integration can be done. We use a new one-step proton exchange procedure, called "soft proton exchange" (SPE) [23], working with a low-acidity mixture of benzoic acid and lithium benzoate. During this process, some lithium atoms (a fraction x) are replaced by protons as described by the following reaction:

$$\mathrm{LiNbO_3} + x\mathrm{H^+} \rightleftharpoons \mathrm{H}_x\mathrm{Li}_{1-x}\mathrm{NbO_3} + x\mathrm{Li^+}. \tag{4}$$

This replacement locally creates a positive index variation of about 0.03 along the aperture of a suitable mask (see Fig. 1). It is important to note that SPE preserves both the non-linear coefficient of the substrate as well as the orientation of the domains.

Our PPLN substrate features a length of 3.2 cm, and the waveguide employed in the experiments has a 1/e width of 6 μm, a 1/e depth of 2.1 μm and a poling period of 12.1 μm. Pumping the sample at a wavelength of 657 nm, degenerate collinear quasi-phase-matching is obtained for photons at a temperature of 100 °C. The temperature is high enough to avoid photorefractive effects. Waveguide-losses at 1 310 nm wavelength are smaller than 0.5 dB/cm. A typical spectrum of the parametric fluorescence in the case of a coherent pump is shown in Figure 2. The degenerate down-converted twin-photons feature a bandwidth of about 40 nm FWHM.

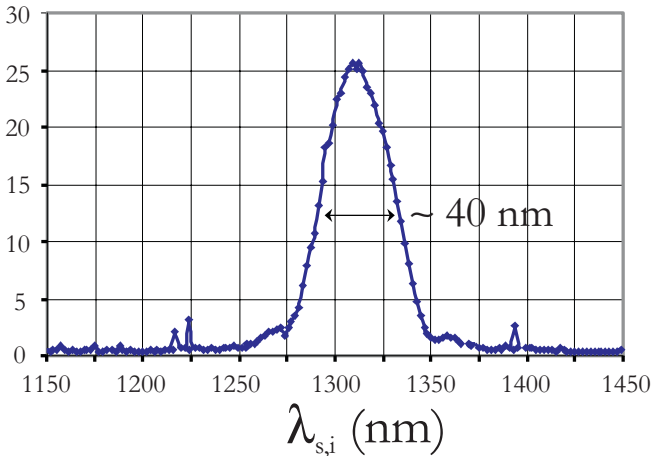

Fig. 2. Measured spectrum for signal and idler photons in case of degenerate phase-matching.

3 Efficiency of the source

3.1 Coincidence counting experiment using a CW pump

As reported recently [1], our new source shows a very high conversion efficiency. In the following, we briefly present the experimental setup and review the major results.

As shown in Figure 3, the waveguide is pumped by a CW laser. After absorption of the remaining pump photons by a filter, signal and idler are separated using a 50/50 single mode fiber optical beam-splitter. The photons are directed to passively quenched LN_2 cooled germanium avalanche photodiodes (Ge–APDs), operated in Geiger mode and featuring quantum efficiencies of

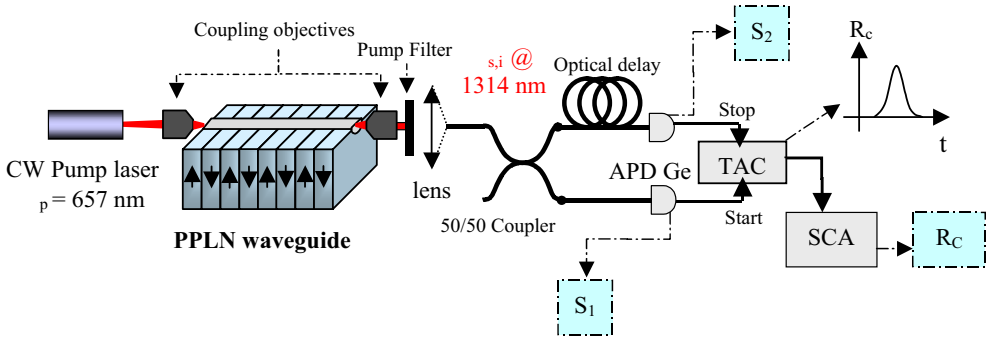

Fig. 3. Schematics to characterize the downconversion efficiency of our PPLN waveguide.

about 10%. Net single count rates are denoted by S_1 and S_2, respectively. The output from the APDs provide the start and stop signals for a time to amplitude converter (TAC) that records a coincidence histogram. A single channel analyzer (SCA) enables counting the coincidence rate R_C in a given time-window.

As shown in [1], the conversion efficiency η can be expressed in terms of the experimental figures S_1, S_2 and R_C (all are net count rates after subtraction of noise), the pump power P_P, the pump wavelength λ_P and the usual constants h (Planck) and c (speed of light)

$$\eta = \frac{N}{N_P} = \frac{S_1 S_2}{2R_C} \frac{hc}{P_P \lambda_P} \,. \tag{5}$$

N and N_P denote the number of photon-pairs created and the number of pump photons injected per second in the waveguide, respectively. The factor of 2 in the denominator takes account of the fact that only 50% of the pairs are split at the beam-splitter. Note that the calculation of the conversion efficiency is based only on easily measurable quantities and does not rely on the inexactly known coupling constants and quantum efficiencies of the detectors. With $P_P \approx 1$ μW measured at the output of the waveguide, $\lambda_P = 657$ nm, $S_i \approx 150$ kHz, and $R_C \approx 1\,500$ Hz, we find a conversion efficiency of about 2×10^{-6}. This is at least 4 orders of magnitude more than the efficiencies calculated for bulk sources recently developed in Geneva [8], in Los Alamos [9] and in Vienna [14]. Note that η is given for one spatial mode (defined by the single mode fibers) but is not normalized to the spectral bandwidth.

3.2 Coincidence counting experiment using a pulsed pump

We now replace the continuous pump by a pulsed laser creating 400 ps pulses at a repetition rate of 80 MHz. Using a mean pump power of only a few μW, the number of pump photons injected per pulse in the waveguide is larger than 10^6. Therefore, taking into account the efficiency of the PPLN waveguide, the probability to create two pairs within the same pump pulse is not negligible. Obviously, the same holds for two pairs originating from two subsequent pump pulses. Exact knowledge of this probability is very important – the creation of two pairs within the same pump pulse is at the heart of quantum teleportation [10], entanglement swapping [21] and generation of GHZ states [19,20] and threatens the security of quantum cryptography systems based on "single photons" produced by PDC [24].

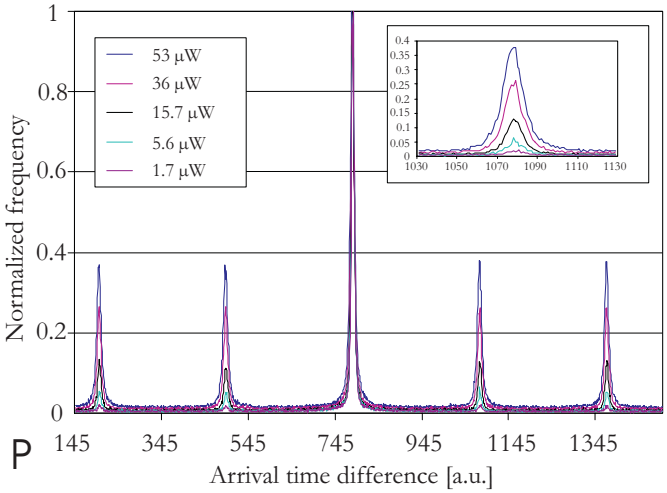

Fig. 4. Central and satellite coincidence peaks as measured with a pulsed pump.

Figure 4 shows typical coincidence histograms for different mean pump power. In opposition to the CW case where only one coincidence peak can be observed, we find a central peak surrounded by equally spaced satellite peaks. The time difference between neighboring peaks is 12.5 ns (corresponding to the 80 MHz repetition rate of the pump laser), and the ratio of the respective magnitudes increases with the mean pump power.

Here we will give only an intuitive explication for the emergence of these satellite peaks. A complete characterization will be presented elsewhere. Since the probability to detect a down-converted photon is far from unity, we will for instance find cases where the photon providing the start signal was created by a pump photon arriving at time t_0, and where the stop-signal originates not from the simultaneously generated idler photon but from a photon generated by the subsequent pump pulse. This coincidence will be located in the first coincidence satellite peak next to the central peak. Since at least two photon-pairs have to be created in order to observe such an event, the ratio

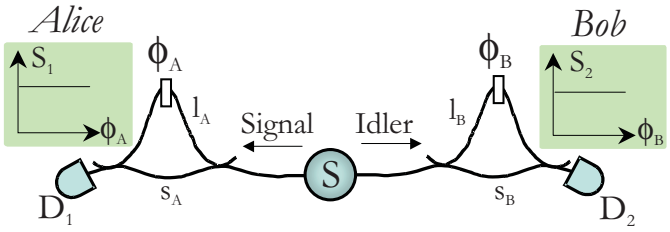

Fig. 5. Schematics of a Franson-type setup to measure 2-photon interferences with energy-time entangled photons. In our case the source S is composed by the CW laser, the PPLN waveguide and a 50/50 beam splitter.

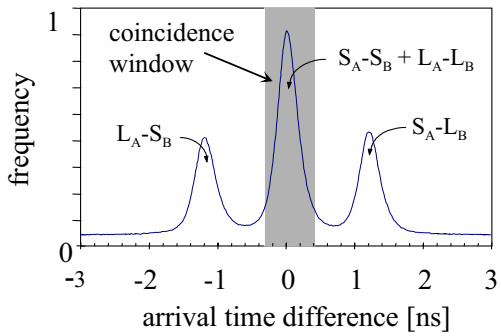

Fig. 6. The coincidence histogram shows three different coincidence peaks, depending on the arms chosen in the interferometers. The events where both photons pass through the same arms ($s_A - s_B$ and $l_A - l_B$) are indistinguishable, leading to photon-pair interference. They can be discriminated from the non-interfering possibilities $l_A - s_B$ and $s_A - l_B$ by means of a single channel analyzer (coincidence window). s and l denote the short and long arms in (A)lice's and (B)ob's interferometers, respectively.

of the magnitude of a satellite peak to central peak (where the creation of only one pair is sufficient) depends, in addition to the detectors' quantum efficiency, on the probability to create a photon pair. It is thus possible to infer this very important property from a simple coincidence measurement.

4 Energy-time entanglement

Apart from featuring a high down-conversion-efficiency, a two-photon source for quantum communication must be able to create *entangled* photons. One possible way to infer the two photon quantum state would be to reconstruct its density matrix [25]. Another possibility is to perform a Bell-type experiment and to infer the degree of entanglement *via* the measured two-photon interference visibility.

The required setup for a test of Bell inequalities for energy-time entangled photon pairs was proposed by Franson in 1989 [26] and first experiments were reported in 1992 [5,6]. A schematic is shown in Figure 5. The source S is composed of a CW laser diode with large coherence length ($\lambda_P = 657$ nm), the PPLN waveguide to create photon-pairs and a fiber optical 50/50 beam-splitter used to separate the twins. The photons are then sent to two analyzers at Alice's and Bob's sides – equally unbalanced Mach-Zehnder type interferometers made from standard telecommunication optical fibers and Faraday mirrors (for a more complete characterization, see [8]). As in the coincidence counting experiment, the detection is made by LN_2 cooled Ge–APDs D_1 and D_2. Note that two detectors are sufficient to record the two-photon fringe visibility.

As the arm length difference (D_L, about 20 cm of optical fiber) is several orders of magnitude larger than the coherence length of the single photons, no single photon interference is observed at the outputs of the interferometers. The single count rates S_1 and S_2, respectively, are independent of the phases ϕ_A and ϕ_B. However, if the coherence length of the pump laser is larger than D_L, an "optical-path" entangled state can be produced where either both down-converted photons pass through the short arms or both through the long arms of the interferometers. The non-interfering possibilities (the photons pass through different arms) can be discarded using a high resolution coincidence technique [27] (see Fig. 6), enabling

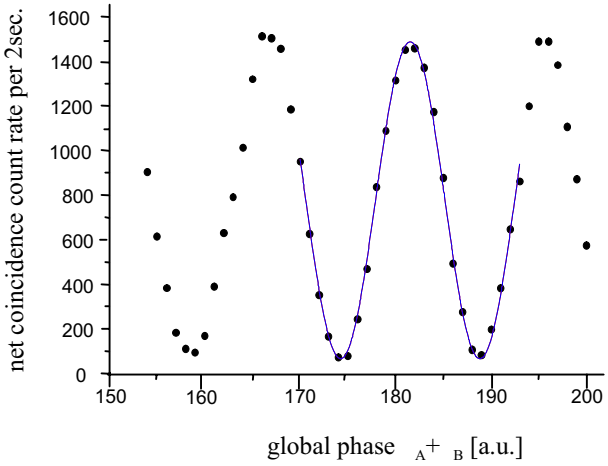

Fig. 7. 2-fold coincidence count rates as measured with energy-time entangled photons. The net visibility is of 97%.

thus to observe quantum correlation with a visibility of theoretically 100%.

Figure 7 shows the coincidence count rates per 2 s while varying the temperature (hence phase) in Alice's interferometer. Although the single count rates do not show any interference, the coincidence count rates are described by a sinusoidal function with a raw fringe visibility of $(92 \pm 1)\%$, and a net visibility (after subtraction of accidental coincidences) of $(97 \pm 1)\%$. Note that the latter are *not* due to a reduced purity of the created entanglement but to the combination of high pair creation rate, losses, and small detector quantum efficiencies. Therefore, in order to characterize the performance of the *source*, it is necessary to refer to the visibility V_{net} after subtraction of accidental coincidences. Since this visibility is close to the theoretical value of 100%, we can conclude that the created state is indeed not far from a pure, maximally entangled state. In addition, we can infer from V_{raw} to a violation of Bell inequalities by 21 standard deviations. To do

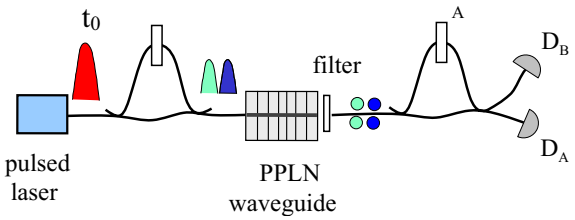

Fig. 8. Experimental setup to create and measure time-bin entangled photon pairs.

so, we have to assume that the other three (not-recorded) coincidence count rates show a similar behaviour and that all coincidence count rates depend only on the sum of the phases.

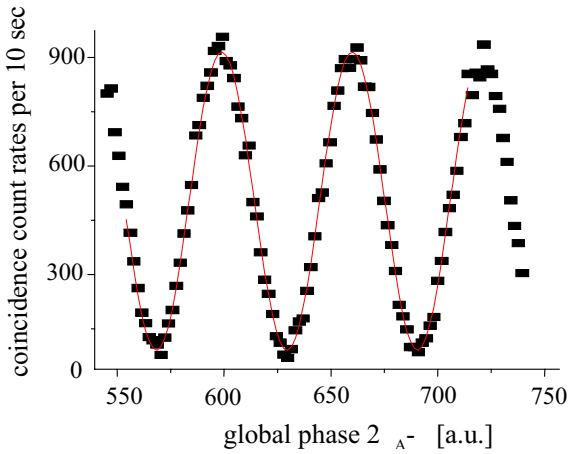

Fig. 9. 3-fold coincidence count rates as measured with time-bin entangled photons. The visibility is of 84%.

5 Time-bin entanglement

As already mentioned in the previous section, the coherence length of the pump photons has to be longer than the path-length difference of the Mach-Zehnder interferometers in order to create an entangled state. Obviously, if we want to pump our non-linear crystal with a pulsed laser, this coherence will be lost. The way to recreate the coherence to the system is to place a third interferometer in the optical path of the pump photons as shown in Figure 8. A short light pulse emitted at a time t_0 enters the pump interferometer having a path-length difference greater than the duration of the pulse. The pump pulse is then split into two pulses of smaller amplitudes following each other with a fixed phase relation. Pumping the PPLN waveguide, we therefore create time-bin entangled photons in a state of the form

$$|\psi_{\mathrm{s,i}}\rangle = \frac{1}{\sqrt{2}}\left(|s\rangle_{\mathrm{s}}|s\rangle_{\mathrm{i}} + \mathrm{e}^{\mathrm{i}\phi}|l\rangle_{\mathrm{s}}|l\rangle_{\mathrm{i}}\right) \qquad (6)$$

where $|s\rangle$ and $|l\rangle$ denote the short or long arm of the first interferometer [28]. Depending on the phase ϕ, it is possible to obtain two out of the four so-called Bell states. The two remaining Bell states can in principle be created using optical switches and delay lines. Finally, choosing different amplitudes for the long and short components in the "pump" interferometer leads to the creation of non-maximally entangled states.

The pulsed laser used in the experiment is the same as the one used in the coincidence counting experiment discussed in Section 3.2. However, a grating reduces the spectral width from 3 to 0.2 nm. Nevertheless, the pulse length remains 400 ps, still longer than the one expected from the Fourier transformation of the spectral width. The interferometer acting on the pump pulse is made from single mode optical fibers at 655 nm wavelength, and the transmission probabilities *via* the long and short arm are the same in order to create maximally entangled states. The energy per pump pulse is low enough to ensure that the creation of more than one photon-pair at a time can be neglected. Finally, the photons are analyzed in a way similar to the one described before. However, for simplicity, both photons are sent into the same interferometer and coincidences are recorded between the two different output ports.

If we look at the coincidence events registered by a TAC placed between D_{A} and D_{B}, we find again three peaks denoting the different paths taken by the signal and idler photons. However, the $s_{\mathrm{A}} - s_{\mathrm{B}}$ and the $l_{\mathrm{A}} - l_{\mathrm{B}}$ events registered in the central peak can now be due to photon-pairs created by a pump photon passed trough either the short or the long arm of the pump interferometer. Therefore the central peak includes four possibilities: $s_{\mathrm{P}} - s_{\mathrm{A}} - s_{\mathrm{B}}$, $l_{\mathrm{P}} - s_{\mathrm{A}} - s_{\mathrm{B}}$, $s_{\mathrm{P}} - l_{\mathrm{A}} - l_{\mathrm{B}}$ and $l_{\mathrm{P}} - l_{\mathrm{A}} - l_{\mathrm{B}}$. Since $s_{\mathrm{P}} - s_{\mathrm{A}} - s_{\mathrm{B}}$ and $l_{\mathrm{P}} - l_{\mathrm{A}} - l_{\mathrm{B}}$ are distinguishable from the two other possibilities by the time between emission of a pump pulse to detection at D_{A} or D_{B}, the coincidence visibility as observed with a SCA is limited to 50%.

To regain the maximum visibility, one has to take into account the emission time of the pump photon by recording three-fold coincidences between the detection of the two down-converted photons and the emission time of the pump pulse. In this way, only the indistinguishable paths $l_{\mathrm{P}} - s_{\mathrm{A}} - s_{\mathrm{B}}$ and $s_{\mathrm{P}} - l_{\mathrm{A}} - l_{\mathrm{B}}$ remain, and the visibility can be increased to 100%.

Figure 9 shows the triple coincidence count rates per 10 s obtained while changing the phase in one interferometer. The raw as well as the corrected net fringe visibilities are of around 84%[2]. This is still higher than the limit of 71% given by Bell inequalities, however, much lower than the maximally achievable value of 100%. The reason for the missing 16% is not yet understood: it is not clear whether the reduced visibility is due to an alignment problem in one of the interferometers, chromatic dispersion effects in the optical fibers or to a phenomenon related to the PPLN waveguide.

[2] Thanks to the threefold coincidence required for each event, accidental coincidences can be neglected.

6 Conclusion and outlook

In this paper we have investigated the performance of a quasi-phase-matched PPLN waveguide for quantum communication. In a CW coincidence counting experiment we first demonstrated a conversion efficiency of 2×10^{-6}, corresponding to an improvement of 4 orders of magnitude compared with bulk configurations. This high efficiency engenders a significant probability of generating more than one photon-pair at a time, even when working with low power laser diodes. We have pointed out a simple means to deduce this probability from the magnitudes of different coincidence count rates as observed in the case of a pulsed pump. In addition to a high down-conversion efficiency, we observed a net visibility of 97% in a Franson-type test of energy-time entangled photon-pairs, demonstrating the high purity of entanglement. This result together with the high conversion efficiency demonstrates the huge potential of PPLN waveguides for future quantum communication sources. Finally, we observed a two-photon visibility of 84% in the case of time-bin entangled pairs. The reason for the limited visibility is not yet understood, but we hope to improve the performance of the source and to make it a key element for future experiments where high photon-pair production rates remain the critical point.

Efforts are underway to develop new PPLN waveguides enabling down-conversion from 710 nm to 1 310 and 1 550 nm, or generating signal and idler photons emitted in opposite directions. This requires different poling periods than the one used for the present work. Finally, a very interesting extension of the PPLN waveguide is to build all-pigtailed devices, or devices where the whole photon-pair source including interferometer and coupler to separate the entangled photons is integrated on a single chip. This could open the way to integrated quantum optics.

We acknowledge financial support by the Cost Action P2 "Application of non-linear optical phenomena" and the ESF "Quantum Information Theory and Communications" as well as the Swiss FNRS and the IST-FET "QuComm" project of the European Commission, partly financed by the Swiss OFES.

References

1. S. Tanzilli, H. De Riedmatten, W. Tittel, H. Zbinden, P. Baldi, M. De Micheli, D.B. Ostrowsky, N. Gisin, Electron. Lett. **37**, 26 (2001).
2. J.S. Bell, Physics **1**, 195 (1964).
3. Z.Y. Ou, L. Mandel, Phys. Rev. Lett. **61**, 50 (1988).
4. Y.H. Shih, C.O. Alley, Phys. Rev. Lett. **61**, 2921 (1988).
5. J. Brendel, E. Mohler, W. Martienssen, Europhys. Lett. **20**, 1923 (1992).
6. P.G. Kwiat, A.M. Steinberg, R.Y. Chiao, Phys. Rev. A **47**, R2472 (1993).
7. G. Weihs, T. Jennewein, C. Simon, H. Weinfurter, A. Zeilinger, Phys. Rev. Lett. **81**, 5039 (1998).
8. W. Tittel, J. Brendel, H. Zbinden, N. Gisin, Phys. Rev. Lett. **81**, 2495 (1998).
9. P.G. Kwiat, E. Waks, A.G. White, I. Appelbaum, P.H. Eberhard, Phys. Rev. A. **60**, R773 (1999).
10. D. Bouwmeester, J.-W. Pan, K. Mattle, M. Eibl, H. Weinfurter, A. Zeilinger, Nature **390**, 575 (1997).
11. D. Boschi, S. Branca, F. De Martini, L. Hardy, S. Popescu, Phys. Rev. Lett. **80**, 1121 (1998).
12. Y.-H. Kim, S.P. Kulik, Y. Shih, Phys. Rev. Lett. **86**, 1370 (2001).
13. T. Jennewein, J.-W. Pan, G. Weihs, A. Zeilinger, Phys. Rev. Lett. **88**, 017903 (2002).
14. T. Jennewein, C. Simon, G. Weihs, H. Weinfurter, A. Zeilinger, Phys. Rev. Lett. **84**, 4729 (2000).
15. D.S. Naik, C.G. Peterson, A.G. White, A.J. Berglund, P.G. Kwiat, Phys. Rev. Lett. **84**, 4733 (2000).
16. W. Tittel, J. Brendel, N. Gisin, H. Zbinden, Phys. Rev. Lett. **84**, 4737 (2000).
17. A. Migdall, Physics Today, 41 (January, 1999).
18. N. Gisin, J. Brendel, H. Zbinden, in *Proceedings symposium on optical fiber measurements*, NIST Boulder Colorado, September 1998, p. 35.
19. D. Bouwmeester, J.-W. Pan, M. Daniell, H. Weinfurter, A. Zeilinger, Phys. Rev. Lett. **82**, 1345 (1999).
20. J.-W. Pan, D. Bouwmeester, M. Daniell, H. Weinfurter, A. Zeilinger, Nature **403**, 515 (2000).
21. J.-W. Pan, M. Daniell, S. Gasparoni, G. Weihs, A. Zeilinger, Phys. Rev. Lett. **86**, 4435 (2001).
22. K. Sanaka, K. Kawahara, T. Kuga, Phys. Rev. Lett. **86**, 5620 (2001).
23. L. Chanvillard, P. Aschieri, P. Baldi, D.B. Ostrowsky, M. De Micheli, L. Huang, D.J. Bamford, Appl. Phys. Lett. **76**, 1089 (2000).
24. N. Lütkenhaus, Phys. Rev. A **61**, 052304 (2000).
25. A.G. White, D.F.V. James, P.H. Eberhard, P. Kwiat, Phys. Rev. Lett. **83**, 3103 (1999).
26. J.D. Franson, Phys. Rev. Lett. **62**, 2205 (1989).
27. J. Brendel, E. Mohler, W. Martienssen, Phys. Rev. Lett. **66**, 1142 (1991).
28. J. Brendel, W. Tittel, H. Zbinden, N. Gisin, Phys. Rev. Lett. **82**, 2594 (1999).